Polymer Chemistry

ROYAL SOCIETY OF CHEMISTRY

PAPER

View Article Online
View Journal | View Issue

Check for updates

Cite this: *Polym. Chem.*, 2026, **17**, 2340

Mechanochemical strategies for the catalytic upcycling of polyethylene *via* transfer hydrogenation

Antonio Cosimo Pio Trimboli, [a] Emilia Paone, [a] Andrea Donato,[a] Riccardo Pellegrini,[b] Elena Groppo, [c] Maximilian Wohlgemuth, [d] Sven Grätz, [d] Francesco Mauriello *[a] and Lars Borchardt *[d]

The development of innovative catalytic strategies is crucial to advance the sustainable upcycling of plastic waste. In this work, we present a mechanocatalytic approach for the selective depolymerization of low-density polyethylene (LDPE) into liquid hydrocarbons using 2-propanol as both direct hydrogen donor and liquid-assisted grinding (LAG) agent and potential radical-quenching medium. High-energy milling was carried out in the presence of a commercial Ru/Al_2O_3 catalyst across four distinct mechanochemical platforms: mixer mill, planetary mill, resonant acoustic mixer and a vibratory disc mill. The influence of mechanical energy input on polymer conversion and product distribution was systematically investigated. Remarkably, under optimized conditions over 95% of the GC-detectable volatile products fall within the C5–C20 range, suitable for fuels and chemical feedstocks. Quantitative GC analysis revealed that 0.47 mg of C5–C20 products (0.188 wt% of the initial polymer) belong to the GC-detectable volatile fraction under optimized conditions. These findings highlight the potential of mechanocatalysis to drive selective valorization of polyolefin wastes under mild, H_2-free conditions by coupling mechanical activation with *in situ* hydrogen transfer.

Received 3rd February 2026,
Accepted 8th May 2026

DOI: 10.1039/d6py00117c

rsc.li/polymers

Open Access Article. Published on 12 Mei 2026. Downloaded on 12/06/2026 20:59:30.
This article is licensed under a Creative Commons Attribution 3.0 Unported Licence.

Introduction

Global plastics production surpassed 400 million tonnes in 2023, with Europe contributing approximately 12.3% (≈54 million tonnes). Despite increasing efforts to enhance sustainability across the value chain, the contribution of circular sources, including mechanically or chemically recycled post-consumer plastics and bio-based alternatives, remains disappointingly marginal. In Europe, only 13.2% of plastics derive from mechanically recycled materials, while chemical recycling contributes a mere 0.2%.[1]

Among synthetic polymers, polyethylene (PE) stands out due to its massive production volume and ubiquitous applications. Most PE products have short lifespans and rapidly accumulate as waste, yet their recycling remains a formidable challenge. Conventional mechanical recycling struggles with mixed or degraded PE waste and typically yields products with downgraded properties unsuitable for high-value applications.[2] Chemo-catalytic valorization, while promising, is still dominated by energy-intensive thermal cracking processes operating at 300–1200 °C with limited selectivity. Reductive catalytic strategies offer milder alternatives but still require temperatures above 200 °C, noble metal catalysts, and high-pressure molecular hydrogen, which introduces logistical and safety concerns.[3,4]

To overcome these limitations, recent efforts have focused on developing depolymerization pathways that operate under milder conditions and intrinsically safer conditions. Hydrogen-transfer catalysis using donor solvents provides an attractive alternative to high-pressure molecular hydrogen.[5] In this context, some of the authors recently demonstrated that 2-propanol (2-PrOH) can efficiently serve as both reaction medium and *in situ* hydrogen source in the reductive upcycling of PE over Ru/Al_2O_3, achieving 65% polymer conversion with high selectivity toward jet fuel and gasoline fractions, while minimizing undesired gas formation.[6] This dual role underscores the practical advantages of H-transfer strategies for polyolefin (PO) upgrading.

Concurrently, mechanochemistry has emerged as a powerful tool for ambient-temperature depolymerization of POs, offering a compelling alternative to conventional

[a]*Dipartimento di Ingegneria Civile, Energia, Ambiente e Materiali (DICEAM), Università degli Studi Mediterranea di Reggio Calabria, Via Zehender (già via Graziella) – Loc. Feo di Vito, I-89123 Reggio di Calabria, RC, Italy*
[b]*Chimet S.p.A., Via di Pescaiola n. 74, I-52041 Viciomaggio, AR, Italy*
[c]*Department of Chemistry, NIS Centre and INSTM, Università degli Studi di Torino, Via Quarello n. 15, I-10135 Torino, Italy*
[d]*Inorganic Chemistry I, Ruhr-Universität Bochum, Universitätsstrasse 150, 44801 Bochum, Germany. E-mail: lars.borchardt@rub.de*

This journal is © The Royal Society of Chemistry 2026

Open Access Article. Published on 12 Mei 2026. Downloaded on 12/06/2026 20:59:30.
This article is licensed under a Creative Commons Attribution 3.0 Unported Licence.

thermochemical approaches.[7–11] Mechanical force can activate inert C–C bonds in PE, generating alkyl radicals that initiate degradation even in the absence of external heating or noble metals. For instance, surface-functionalized grinding media, such as sulfated or redox-active zirconia spheres, have enabled the conversion of POs into C1–C10 hydrocarbons *via* radical pathways, bypassing the need for powder catalysts and thermal input.[12] Similarly, ball milling of PE with water has been shown to induce C–C bond cleavage and generate a diverse mixture of alkanes, alkenes, alcohols, and ketones, with over 80% carbon conversion, using only Al_2O_3 as a co-milling agent.[13] These studies demonstrate the versatility of mechanochemistry in activating inert POs under mild conditions and without noble metals. However, they primarily rely on radical or hydrolytic mechanisms, often yielding broad product distributions and limited control over selectivity toward targeted hydrocarbon fractions.[14–21] Several catalytic strategies for polyethylene (PE) upcycling have been developed in recent years, aiming at transforming this recalcitrant polymer into fuels or value-added chemicals. Notably, Hartwig and Guironnet independently reported tandem isomerization–metathesis approaches enabling the selective conversion of polyethylene into propylene.[22,23] While highly elegant and selective, these processes require elevated temperatures, well-defined homogeneous catalytic systems, and continuous removal of light olefins to shift the equilibrium. In a different approach, Lercher and co-workers demonstrated that polyethylene can be cracked in ionic-liquid-based systems, where strong Brønsted acidity and thermal activation promote C–C bond scission within the polymer backbone.[24] Although effective, these methods remain intrinsically thermally driven and rely on high-temperature operation to achieve meaningful conversion. Despite these important advances, strategies that explicitly couple mechanical activation with catalytic stabilization under mild, hydrogen-free conditions remain largely unexplored.

In contrast, this work introduces a hybrid strategy for the reductive upcycling of low-density polyethylene, which combines mechanochemical activation with hydrogen-transfer catalysis, using 2-PrOH as a direct hydrogen donor and commercially available Ru/Al_2O_3 (5 wt% – Chimet S.p.A) as the heterogeneous catalyst (Fig. 1). It should be noted that the energy-efficiency considerations discussed herein are intended as an internal comparison among the different mechanochemical platforms and catalytic configurations investigated in this study. Conventional batch hydroconversion of polyethylene typically requires temperatures above 200 °C, pressurized hydrogen, and extended reaction times, with substantial energy contributions arising from heating, agitation, and hydrogen compression.[3] In contrast, the present mechanochemical approach operates at ambient temperature and atmospheric pressure, delivering energy directly into bond activation through mechanical forces. A quantitative cross-platform energy benchmarking against thermal reactors lies outside the scope of this work and will be addressed separately. While previous studies have explored either mechanochemical depolymerization or catalytic hydrogen-transfer separately, this is the first systematic investigation of how different mechanocatalytic platforms modulate the efficiency and selectivity of reductive upcycling of PE. By comparing four distinct milling technologies: (i) mixer mill, (ii) planetary mill, (iii) vibratory disc mill and (iv) resonant acoustic mixer, we aim to elucidate how different mechanochemical systems influence polymer conversion and product selectivity, targeting valuable fuel-range hydrocarbons such as gasoline, jet fuel, diesel and lubricants. This integrated approach allows to elucidate how mechanical energy profiles influence the formation of targeted hydrocarbon fractions, offering a scalable and energy-efficient strategy for catalytic plastic upcycling.

Experimental

Materials, catalyst synthesis and characterization

All chemicals, including low-density polyethylene (LDPE – $M_n \approx 1700$, $M_w \approx 4000$), were purchased from commercial source. The commercial Ru/Al_2O_3 (5 wt%) catalyst, provided by Chimet S.p.A., was synthesized by a deposition–precipitation method similar to that described in ref. 25–27 using ruthenium recovered from industrial waste. It was used as received without any pretreatment, except for drying overnight at 90 °C prior to use. It features highly dispersed rutile-like RuO_2 nanoparticles (~1.5 nm) on an industrial alumina (surface area = 121 $m^2\ g^{-1}$, pore volume 0.43 $cm^3\ g^{-1}$, mixture of δ and θ phases). The RuO_2 phase undergoes complete reduction to metallic Ru below 150 °C, with ~33% of metal dispersion measured by pulsed CO chemisorption. The combination of Lewis-acidic alumina support and easily reducible RuO_2 nanoparticles makes it highly favorable for hydrogen-transfer driven upgrading of POs.[6,28]

Catalytic tests and products analysis

For the catalytic upcycling of LDPE, four different mechanochemical devices were employed: (i) Retsch MM-500 vario ball mill; (ii) Fritsch P7 planetary mill; (iii) Retsch RS 300 vibratory disc mill; (iv) resonant acoustic mixer (RAM) LabRAM II by Resodyn. Zirconium oxide milling balls (Type ZY-S, ∅ = 10 mm, average weight 3.2 g) were purchased from Sigmund Lindner GmbH.

In a typical procedure, commercial LDPE and Ru/Al_2O_3 catalyst were combined in 40 : 1 mass ratio, along with the desired hydrogen donor. The polyethylene loading was 250 mg per 10 mL of jar volume. The mixtures were loaded into milling jars of different volumes (10 mL for the MM-500, 20 mL for the P7, 50 mL for the RS 300, and 10 mL for the RAM II), while ensuring identical fill factors across all systems. Milling was carried out under ambient atmosphere.

After completion of the mechanochemical treatment, soluble products were extracted directly from the milling jars by adding dichloromethane (DCM, Sigma-Aldrich, 99.8%): 2 mL for the MM-500 and RAM II, 4 mL for the P7, and 10 mL for the RS 300. Extraction was assisted by agitation: 1 min at 10 Hz (MM-500), 1 min at 100 rpm (P7), 1 min at the default

Open Access Article. Published on 12 Mei 2026. Downloaded on 12/06/2026 20:59:30.
This article is licensed under a Creative Commons Attribution 3.0 Unported Licence.

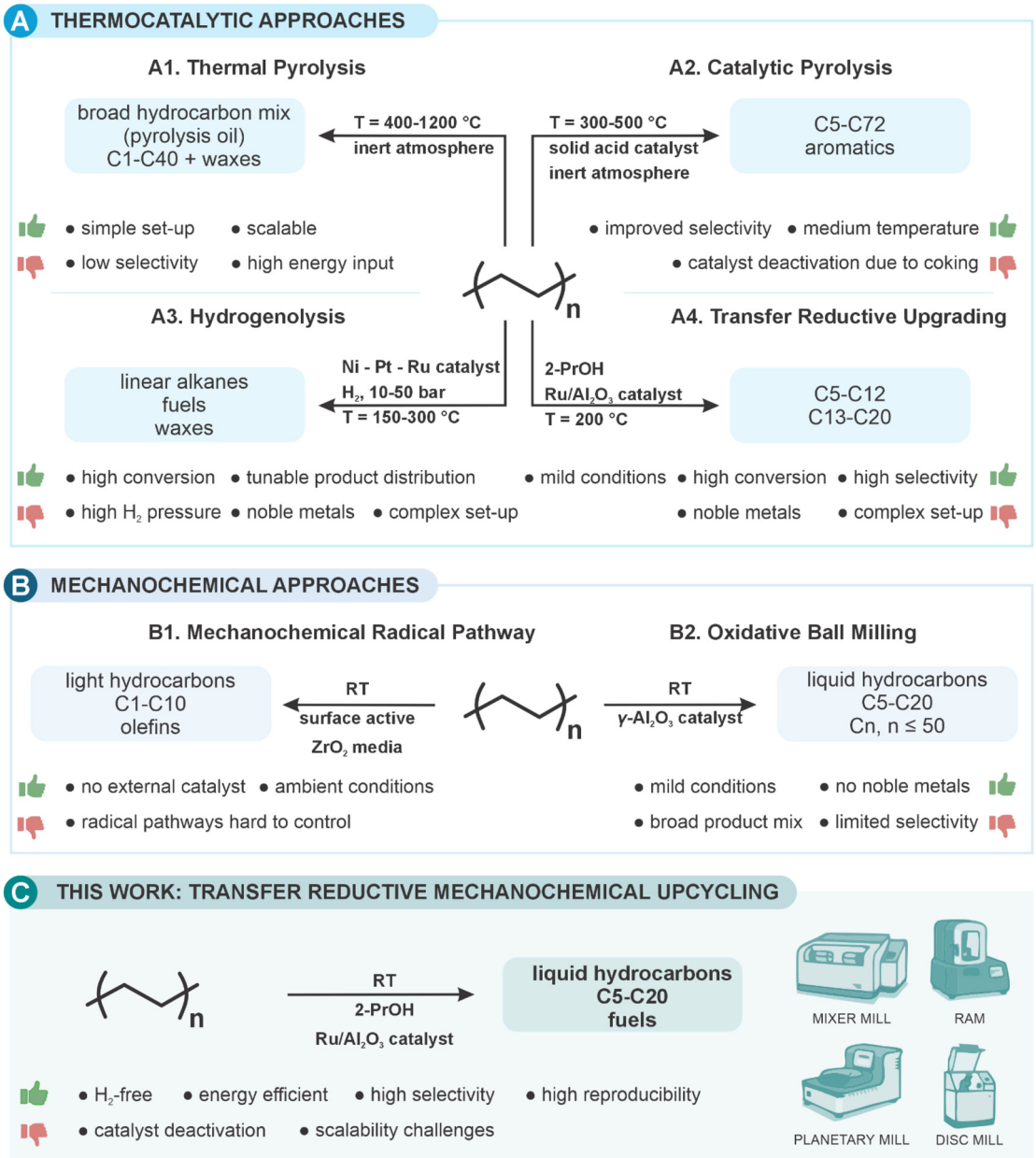

Fig. 1 (A) Thermocatalytic strategies for the reductive upcycling of polyethylene; (B) mechanochemical approach for the catalytic upcycling of polyethylene; (C) comparative overview of mechanocatalytic systems applied in the upcycling of polyethylene by using 2-propanol as H-donor source and as liquid-assisted grinding (LAG) agent: mixer mill, resonant acoustic mixer, planetary mill and vibrating disc mill.

frequency (RS 300), and 1 min at 20 g (RAM II). The resulting mixtures were vacuum-filtered to separate the liquid phase from the solid residues. The transparent solutions were analyzed by GC-MS, while the solid residues were dried at 80 °C overnight. The amount of unreacted substrate was estimated by subtracting the catalyst mass from the total mass of the recovered solid.

PE conversion was calculated using eqn (1):

$$\text{Conversion}\,(\%) = \left[1 - \frac{m_{(\text{unreacted POs})} - m_{(\text{catalyst})}}{m_{(\text{initial POs mass})}}\right] \times 100 \quad (1)$$

where $m_{(\text{unreacted POs})}$ is the mass of the dried residue after solvent removal and $m_{(\text{initial POs})}$ is the initial mass of plastic introduced into the reactor. The selectivity for a given product i was calculated as in eqn (2):

$$\text{Selectivity}\,(\%) = \frac{A_i}{\sum A_i} \times 100 \quad (2)$$

where A_i is the GC peak area of product i, and $\sum A_i$ is the total area of all identified and quantified products in both gas and liquid phases. It should be emphasized that the selectivity values reported throughout this work are derived exclusively

 This journal is © The Royal Society of Chemistry 2026

Open Access Article. Published on 12 Mei 2026. Downloaded on 12/06/2026 20:59:30.
This article is licensed under a Creative Commons Attribution 3.0 Unported Licence.

from GC–MS analysis and therefore refer only to the volatile and semi-volatile fraction of the product mixture. As a result, these values represent relative distributions within the GC-detectable products and should not be interpreted as absolute mass-based selectivities over the total converted polymer.

Due to the limited amount of 2-propanol employed (500 μL), post-reaction NMR analysis was not accessible after milling and work-up. Nevertheless, previous studies conducted under conditions with an excess of 2-propanol confirmed the formation of acetone by GC-FID, supporting its role as hydrogen donor *via* dehydrogenation under mechanochemical conditions.[5,6] In this context, the α-C–H (methine) and O–H hydrogen atoms of 2-propanol are considered the most likely hydrogen sources involved in the transfer process. In accordance with the literature, only products with carbon numbers up to C50 were considered, based on GC–MS detection limits and boiling points constraints. These compounds were categorized into three fractions: C5–C12 (gasoline range), C13–C20 (diesel/jet fuel range), and >C20 (lubricant/wax range).[29,30] GC–MS analysis was performed using a Shimadzu NEXIS 2030 gas chromatograph equipped with a 30 m × 0.25 mm ID column coated with 5% diphenyl/95% dimethyl polysiloxane, with helium as the carrier gas. The reported carrier gas flow rate of 25 mL min^{-1} refers to the total inlet flow under split injection conditions, while the effective column flow was maintained within the typical range for a 0.25 mm ID capillary column; 5 μL of sample was injected in split mode, and the oven was programmed at 50 °C (1 min hold), then ramped to 250 °C at 20 °C min^{-1} and held for 10 min. The mass spectrometer operated in electron ionization mode (70 eV), with spectra collected over *m*/*z* 40–400, and compound identification was performed by comparison with the NIST (version 11) library.

Complementary MALDI-TOF mass spectrometry analyses were therefore performed to probe the presence of heavier species. Matrix assisted laser desorption ionization time of flight mass spectroscopy (MALDI-TOF) was carried out on a Bruker Autoflex Speed spectrometer using a 337 nm nitrogen laser or on a Bruker Ultraflex 3 with 3,5-dimethoxy-4-hydroxycinnamic Acid as matrix.

Gaseous products were collected in a gas sampling bag and analyzed by GC using a Shimadzu GC-2014 equipped with a flame ionization detector (FID).[31] The columns included a right 12.5 m (l) 3 0.32 mm (i.d.) packed column, which comprised 3 m Hayesep D, 4 m HS, and 2.5 m HN, and a left 2 m (l) 3 0.32 mm (i.d.) 10% Carbowax 20 m Ch packed column. Individual compounds in the liquid fraction were identified by comparison of their mass spectra with those reported in the NIST mass spectral library. After identification, the carbon number of each compound was determined from the corresponding molecular structure, and the detected products were grouped into three fractions according to their carbon number: gasoline (C5–C12), diesel and jet fuel (C13–C20), and lubricant (>C20). Gaseous products were analyzed separately by GC-FID. For these light hydrocarbons, carbon-number regions were assigned based on chromatographic retention behavior. Under the applied conditions on Hayesep and Carbowax packed columns, hydrocarbons elute sequentially with increasing carbon number; therefore, the detected peaks were interpreted according to the expected elution order of homologous *n*-alkanes.

To confirm the dual role of protic solvents as liquid-assisted grinding (LAG) agents and hydrogen donors, ^{1}H NMR analyses were carried out using 2-propanol and deuterated 2-propanol, with spectra recorded on a Bruker Avance III HD spectrometer at 400 MHz and chemical shifts reported in ppm.

Residual PE was removed from the Ru/Al_2O_3 catalyst *via* Soxhlet extraction with refluxing xylene (125 mL, ~138 °C, 16 h), followed by drying at ambient conditions and subsequently at 80 °C for 12 h. The recovered catalyst was then analyzed by scanning electron microscopy (SEM) coupled with energy-dispersive X-ray spectroscopy (EDX) using a JEOL JSM-IT800 microscope operated at 15 kV and equipped with an Oxford Ultim Max silicon drift detector (SDD). SEM micrographs revealed clean catalyst surfaces and no evidence of polymeric residues, confirming the effectiveness of the Soxhlet extraction process.

Results and discussion

Optimization of mechanical parameters without catalyst

To evaluate the influence of only mechanical parameters, preliminary upcycling tests were carried out without catalyst or H-donor, using the four mechanochemical platforms under investigation. Parameters such as milling frequency (MM-500), rotational speed (P7), and acceleration (RAM II) were systematically varied, while the RS 300 vibratory disc mill was operated at its default frequency. All reactions were conducted at room temperature for 60 minutes in zirconia jars, using zirconia milling media: 1 × 10 mm ball (MM-500), 10 × 10 mm balls (P7) and a zirconia disc (RS 300).

Even without catalyst, measurable polymer conversion was observed across all platforms, with selectivity varying with the experimental parameters.

In particular, in the MM-500 mixer mill, increasing the milling frequency led to improved PE conversion and selectivity (Fig. 2B, Table S1 and Fig. S1). The optimal frequency was 30 Hz, yielding 18% conversion and 37% selectivity toward C5–C20 hydrocarbons. Frequencies above 30 Hz resulted in slightly diminshed performance, likely due to excessive mechanical input causing thermal or structural side effects.

In the RAM II resonant acoustic mixer, acceleration was varied from 30 to 90 g (Fig. 2C, Table S2 and Fig. S2). The best results were obtained at 90 g, with 11% conversion and 67% selectivity toward diesel/jet fuel range products. In the P7 planetary mill, rotational speed was varied between 350 and 800 rpm (Fig. 2D, Table S3 and Fig. S3). The most favorable condition was 500 rpm, achieving 11% conversion and 56% selectivity toward C5–C20 fractions. At higher rotational speeds, conversion slightly increases at the expensed of selectivity.

These results collectively demonstrate that increasing mechanical energy (*via* frequency, rotational speed or accelera-

Open Access Article. Published on 12 Mei 2026. Downloaded on 12/06/2026 20:59:30.
This article is licensed under a Creative Commons Attribution 3.0 Unported Licence.

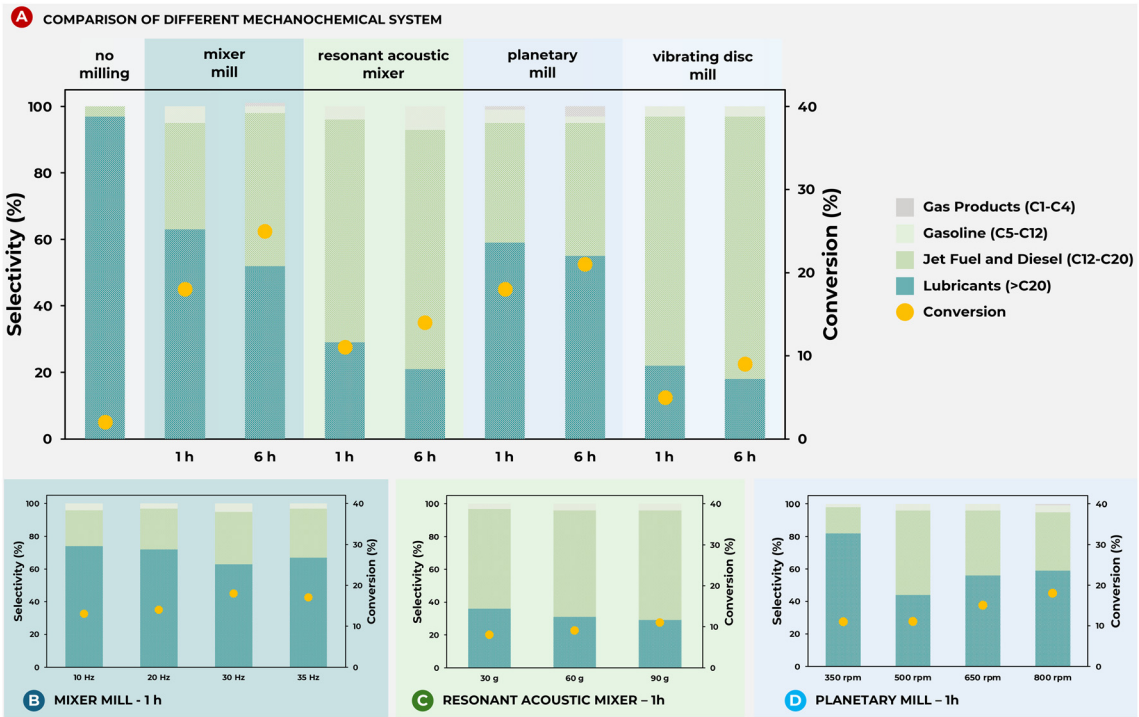

Fig. 2 Influence of mechanical parameters on the PE4000 upcycling (conversion and product selectivity) without catalyst and without H-donor & LAG agent. (A) Comparative performance of the four mechanochemical systems as a function of reaction time (1–6 h). Reaction conditions: room temperature, 1–6 h, no catalyst, no H-donor, 1 × 10 mm zirconia ball for Mixer Mill with 30 Hz frequency, no milling media for Resonant Acoustic Mixer with 90 g acceleration, 10 × 10 mm zirconia ball for Planetary Mill with 800 rpm rotation speed, zirconia disc for Vibrating Disc Mill. (B) Effect of milling frequency in the MM-500 Mixer Mill. Reaction conditions: room temperature, 1 h, no catalyst, no H-donor, 1 × 10 mm zirconia ball. (C) Effect of acceleration in the RAM II Resonant Acoustic Mixers. Reaction conditions: room temperature, 1 h, no catalyst, no H-donor, no milling media. (D) Effect of rotational speed in the P7 Planetary Mill. Reaction conditions: room temperature, 1 h, no catalyst, no H-donor, 10 × 10 mm zirconia balls. Reported selectivity refers exclusively to GC-detectable volatile products.

tion) enhances polymer chain scission and promotes formation of lower-molecular-weight hydrocarbons. However, excessive input may reduce selectivity or induce side reactions, underscoring the need for careful parameter optimization.

To further probe the effect of prolonged activation, reactions were extended up to 6 hours under their optimal conditions for each device (*i.e.* 30 Hz for MM-500, 800 rpm for P7, 912 min^{-1} for RS 300, and 90 g for RAM II, Table S4 and Fig. S4). A control experiment without miling ("no milling") was performed by agitating LDPE with 2 mL of DCM for 1 min at 10 Hz in the MM-500, confirming that solvent-assisted agitation alone has a negligible effect. The results are summarized in Fig. 2A, which compares the effect of the different milling platforms at two different reaction times. The RAM II provided the most favorable distribution toward the targeted <C20 products, highlighting its strong selectivity. The P7 and MM500 showed very similar behavior, both delivering moderate conversion and selectivity, while the RS300 was less effective and biased toward heavier fractions. In all cases, gaseous products remained negligible, confirming the key role of reactor type and milling duration in controlling chain scission and product distribution. Gaseous products remained below 3% in all cases, highlighting the key role of reactor type and milling duration in controlling chain scission and product distribution.

To isolate the effect of the milling assembly on polyethylene activation, the influence of different milling media was systematically evaluated under catalyst-free and hydrogen-donor-free conditions. Zirconia, stainless steel, and PTFE jars and balls were tested under otherwise identical milling parameters. Both stainless steel and zirconia media resulted in nearly identical polymer conversion levels and very similar product distributions, indicating that mechanical energy transfer, rather than the chemical nature of the milling media, governs polymer activation under these conditions. In contrast, PTFE showed negligible activity, confirming that chemical inertness combined with insufficient mechanical impact leads to minimal depolymerization (Table S5 and Fig. S5). Zirconia was therefore selected for all catalytic experiments due to its chemical inertness and the absence of metallic surface activity, which avoids potential interference between steel surfaces and the Ru catalyst and ensures that the observed catalytic effects arise exclusively from the Ru/Al_2O_3 system.

Optimization of reaction conditions with Ru/Al_2O_3 catalyst

Building on the optimization of mechanical parameters across different milling systems, the MM-500 mixer mill was selected

 This journal is © The Royal Society of Chemistry 2026

Open Access Article. Published on 12 Mei 2026. Downloaded on 12/06/2026 20:59:30.
This article is licensed under a Creative Commons Attribution 3.0 Unported Licence.

as the reference system for catalytic tests with Ru/Al_2O_3. Its reproducibility and controllability under optimized conditions (30 Hz, 1 × 10 mm zirconia ball) provided a robust framework to investigate the role of H-donor molecules in PE activation. A systematic screening of H-donor molecules was perfomed (Fig. 3A, Table S6 and Fig. S6). In the absence of any H-donor, conversion was modest (14%), with the majority of products (77%) in the lubricants range, and the remaining in the diesel/jet fuel (21%) and gasoline (2%) range. Methanol and ethanol yielded similar conversions, with selectivity shifting toward lighter hydrocarbons (61% diesel/jet fuel and 4% gasoline). 2-Propanol emerged as the most effective donor, achieving 18% conversion and 80% selectivity toward diesel/jet fuel fractions, along with moderate amounts of gasoline (6%) and lubricants (13%). 2-Butanol delivered intermediate performance, with increased lubricants formation (37%). In all cases, the formation of light gaseous products (C1–C4) remained minimal (<1%).

These results highlight the multifunctional role of alcohols, which act as hydrogen donors, liquid-assisted grinding (LAG) agents, and may also participate in radical-termination processes that stabilize mechanically generated polymer fragments into closed-shell products *via* catalytic hydrogen transfer, rather than through any paramagnetic or spin-related effect. Their presence enhances polymer mobility, stabilizes reactive intermediates, and promotes selective C–C bond scission under mechanochemical conditions. The low gas yield and high liquid selectivity underscore the efficiency of 2-propanol in particular.

As a control experiment to isolate the liquid-assisted grinding (LAG) effect from hydrogen donation, tetrahydrofuran (THF) was tested as a non-hydrogen-donor liquid under otherwise identical mechanochemical conditions (Table S6 and Fig. S6). While THF can act as a grinding aid, it led only to marginal polyethylene conversion and limited formation of liquid-range products. This confirms that LAG effects alone are insufficient to drive effective depolymerization and that hydrogen-donor alcohols play an essential role in the present system. To ascertain the hydrogen-donating role of 2-propanol, ^{1}H NMR analyses were conducted comparing reactions performed with regular and deuterated 2-propanol (2-propanol-d_1) (Fig. S7).

Spectra from reactions with 2-propanol displayed enhanced signals in regions associated with vinylic protons (δ 5.0–5.6 ppm), oxygenated groups (δ 3.9–4.1 ppm) and branched aliphatic structures (and δ 1.0–1.5 ppm). In sharp contrast, these resonances were significantly suppressed in the deuterated system, consistent with a primary kinetic isotope effect and confirming active hydrogen transfer from the donor. GC-MS analyses further supported these findings, revealing a higher abundance of reduced and oxygenated hydrocarbons in the products generated with 2-propanol, compared to its deuterated analogue. The product distribution highlights a pronounced impact of the hydrogen donor on the selectivity of mechanocatalytic polyethylene upcycling (Fig. S8). In the absence of H-donor molecules, the reaction mainly affords linear oxygenated species (>80%), with only minor fractions of non-oxygenated products. The addition of alcohols, however, introduces distinct effects: methanol strongly promotes the formation of branched products, both oxygenated and non-oxygenated (*ca.* 14% each), while reducing the share of linear oxygenates. In contrast, ethanol and 2-propanol yield almost exclusively linear products (≈80% oxygenated), with complete suppression of the branched fractions. The use of 2-butanol leads to an intermediate behavior, increasing the amount of branched oxygenated products (~11%) while still favoring linear oxygenates. These findings suggest that both the steric profile and the hydrogen-transfer ability of alcohols govern not only the oxidation degree but also the branching tendency of the polymer fragments.

Taken together, these results provide compelling molecular-level evidence that hydrogen atoms from 2-propanol are actively transferred to reactive intermediates, thereby promoting C–C bond scission and partial reduction of the polymer backbone. Hence, 2-propanol is not merely acting as a grinding aid but serves as a genuine hydrogen donor, directly

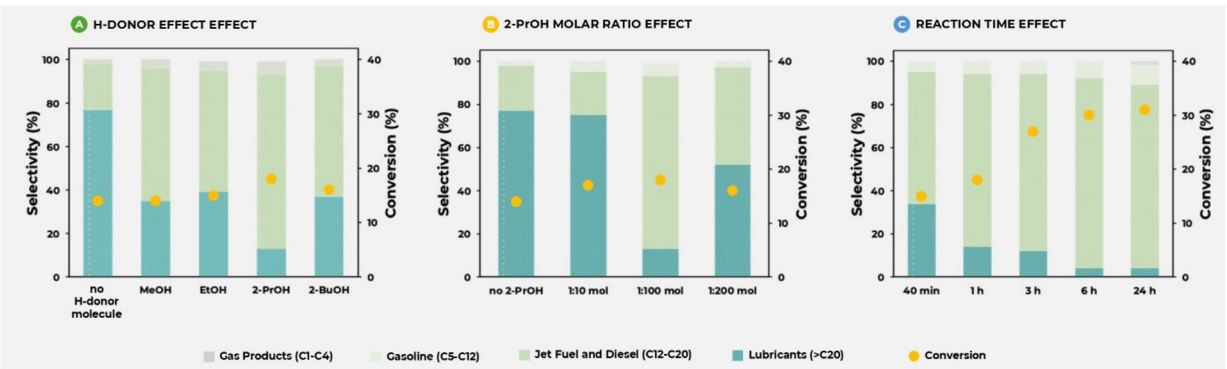

Fig. 3 Effect of (A) the H-donor source, (B) the amount of 2-PrOH (PE/2-PrOH molar ratio), and (C) the reaction time, on the mechanocatalytic upcycling of PE4000 in the presence of Ru/Al_2O_3 catalyst, in terms of both conversion and products selectivity. All reactions were performed using a mixer mill under the following conditions: room temperature, PE/Ru wt% ratio: 40 : 1, 1 × 10 mm zirconica ball, milling frequency = 30 Hz, reaction time = 1–6 h, PE/2-PrOH molar ratio: 1 : 10–1 : 200. Reported selectivity refers exclusively to GC-detectable volatile products.

Open Access Article. Published on 12 Mei 2026. Downloaded on 12/06/2026 20:59:30.
This article is licensed under a Creative Commons Attribution 3.0 Unported Licence.

shaping the extent of PE depolymerization and the distribution of the resulting products.

To probe the involvement of radical intermediates during mechanocatalytic polyethylene degradation, spin-trapping experiments were performed by adding 2,2,6,6-tetramethylpiperidinyloxyl (TEMPO) to the milling batch under otherwise identical reaction conditions. This addition show a marked reduction in polymer conversion (10%) accompanied by prominent signals corresponding to TEMPO itself in GCMS chromatogram, indicating effective radical quenching. To further validate the radical-mediated pathway, additional experiments were conducted using the well-established radical scavenger butylated hydroxytoluene (BHT) (Fig. S9). Similar trends were observed, with a significant suppression of polymer conversion (7%) and a shift in the product distribution toward heavier, less fragmented species. Notably, despite the differences in chemical structure and analytical detectability between TEMPO and BHT, both scavengers produced comparable inhibition effects. This convergence provides strong indirect evidence that macroradicals are generated during mechanical activation and play a central role in the depolymerization process. Together, these results support a radical-mediated depolymerization pathway in which mechanically generated macroradicals are stabilized and evolve *via* Ru-mediated transfer hydrogenation from 2-propanol. This mechanistic insight highlights the synergistic interplay between mechanical activation, Ru active sites, and the oxide support in controlling both polymer scission and product selectivity. Control experiments performed using bare Al_2O_3 confirmed that the support alone exhibits limited activity (14 ± 3.2% conversion) with a product distribution dominated by heavier fractions, consistent with a minor contribution from radical pathways associated with its Lewis acidity (Fig. S10). In contrast, the Ru/Al_2O_3 system promotes higher conversion and a pronounced shift toward mid-distillate products, highlighting the essential role of Ru in enabling efficient hydrogen-transfer processes *via* reducible RuO_2 species. Moreover, the combined use of TEMPO and BHT demonstrates the robustness of the radical-inhibition approach as a tool to interrogate complex mechanocatalytic transformations, providing a solid foundation for future mechanistic studies aimed at optimizing selective polyethylene upcycling. The reaction is interpreted as a mechanoradical-initiated process, where mechanical stress induces C–C bond scission and formation of macroradicals.[12] These intermediates are then converted *via* catalytic hydrogen transfer in the presence of Ru/Al_2O_3 and 2-propanol, in agreement with reported hydrogen-transfer mechanisms.[5,6,27] To further explore the influence of donor concentration, a series of experiments was conducted varying the PE/2-PrOH molar ratio, defined as the ratio between polymer chains (based on the average molecular weight) and 2-propanol molecules (Fig. 3B, Table S7 and Fig. S11). Conversion and selectivity improved with increasing donor concentration, peaking at a 1 : 100 ratio, where conversion reached 18% and the product distribution centered in the diesel/jet fuel range (80%). Beyond this point, dilution effects reduced conversion and shifted selectivity toward heavier fractions. These results confirm the importance of optimizing H-donor loading to balance hydrogen availability and reaction efficiency.

Finally, the effect of reaction time was investigatd under optimal conditions (1 : 100 PE/2-PrOH molar ratio, 30 Hz) (Fig. 3C, Table S8 and Fig. S12). Conversion progressively increased reaching 30% at 6 hours, reflecting progressive polymer chain scission under sustained mechanical and catalytic activation. The product distribution was dominated by diesel/jet fuel fractions (88%), with moderate gasoline (8%) and lubricant (4%) fractions, and negligible gas formation. Longer milling times yielded only marginal improvements in the conversion (31%), without altering the selectivity, suggesting a plateau in catalytic activity.

Catalyst stability and comparative performance across milling platforms

SEM-EDS analysis of the spent Ru/Al_2O_3 catalyst (Fig. S13) provides visual and compositional evidence of progressive catalyst degradation during extended milling. Initially, SEM micrographs reveal well-defined, rounded Ru/Al_2O_3 particles. After 6 h of reaction, these particles appear coated by a continuous layer of material—likely residual polymer or condensed products—suggesting partial encapsulation of the active surface. At 24 h, the catalyst morphology is drastically altered: individual particles are no longer distinguishable, and the surface appears embedded in a lamellar matrix, possibly indicative of pseudo-graphitic carbonaceous deposits.

Elemental mapping corroborates these observations, showing a gradual decrease in Ru, Al, and O content, accompanied by an increase in surface carbon and the appearance of Zr. These changes reveal two concurrent deactivation phenomena: (i) coke deposition, which progressively blocks acive Ru and Al sites essential for C–C bond cleavage and hydrogen transfer, and (ii) zirconia abrasion, which introduces Zr species that contaminate the catalyst surface and further mask active sites. Notably, similar zirconia transfer phenomena have been reported by Weckhuysen and co-workers,[12] who demonstrated that surface-activated zirconia grinding media can participate directly in mechanochemical polyolefins upcycling, even acting as redox-active catalytic interfaces.[6]

The stabilization of liquid yield and the slight decline in selectivity toward middle distillates after 6 h of milling (Fig. 3C, Table S8 and Fig. S13) reflect these fouling and mechanical wear phenomena. These findings identify 6 h as the optimal milling time, balancing conversion, selectivity and catalyst integrity. Beyond this point, further milling primarily accelerates catalyst degradation without significant gains in performance, emphasizing the need for strategies to mitigate mechanical wear mechanocatalytic systems. These observations clearly distinguish short-term catalytic performance under optimized conditions from long-term degradation phenomena occurring upon extended milling, thereby resolving the apparent discrepancy between conversion trends and catalyst stability. Having identifyied 2-propanol as the most effective hydrogen donor and established optimal donor

 This journal is © The Royal Society of Chemistry 2026

Open Access Article. Published on 12 Mei 2026. Downloaded on 12/06/2026 20:59:30.
This article is licensed under a Creative Commons Attribution 3.0 Unported Licence.

loading and reaction time, we proceeded to compare the four mechanochemical platforms under their respective best conditions (Fig. 4, Table S9 and Fig. S14). The mixer mill delivered the highest performance, achieving 30% conversion with a product distribution dominated by diesel/jet fuel fractions (88%), moderate gasoline content (8%), minor lubricants (4%), and negligible gas formation. The planetary mill and RAM systems showed lower conversions (~25%) and a slightly broader product distributions, while the vibratory disc mill was the least effective, providing only 12% conversion and a much broader product distribution.

These results confirm that, after sequential optimization of H-donor, solvent amount, and reaction time, the mixer mill remains the most efficient platform for PE upcycling, combining highest conversion with selective formation of valuable liquid hydrocarbons. The resonant acoustic mixer, while less performant, demonstrated promising selectivity and scalability potential, in line with recent findingd by Makarov *et al.* on the upcycling of PLA using this technology.[32] Comparison across different milling technologies reveals pronounced differences also in product distribution (Fig. S15). The mixer mill produces mainly linear oxygenated species (~74%), with a moderate share of linear non-oxygenates (~22%) and only minor branched products. The resonant acoustic mixer, on the other hand, strongly increases the fraction of branched oxygenated species (~16%) and branched non-oxygenates (~11%), at the expense of linear oxygenates, suggesting a more efficient fragmentation and functionalization pathway. The planetary mill stands out for its unique selectivity: nearly 80% of the products are branched non-oxygenated hydrocarbons, while oxygenated species are largely suppressed—an outcome consistent with its high-energy, shear-dominated regime. By contrast, the vibrating disc mill generates the cleanest distribution, with >85% linear oxygenated products and negligible branched species. Overall, these results highlight how the milling environment—defined by impact *vs.* shear, energy input, and mixing mode—dictates not only the oxidation level but also the branching of the polymer fragments. To assess the applicability of the mechanocatalytic strategy beyond model substrates, a real post-consumer polyethylene waste (PE-RW) was investigated and directly compared with model polymers of different molecular weights (PE4000 and UHMWPE) under the optimized conditions (Ru/Al_2O_3, MM500, 30 Hz, 6 h, 1 : 100 mol ratio PE : 2-PrOH).

As summarized in Fig. 5, the system exhibits a remarkably consistent catalytic activity across all substrates, with comparable conversions ranging from 27 to 30%, indicating that the overall extent of depolymerization is only weakly affected by polymer origin or molecular weight.

In contrast, pronounced differences emerge in the product distribution. Low-molecular-weight PE4000 predominantly yields middle-distillate hydrocarbons in the jet fuel and diesel range (C13–C20, 88%), with only minor contributions from lubricant-range products (>C20, 4%) and gasoline fractions (C5–C12, 8%). Conversely, UHMWPE displays a clear shift toward heavier hydrocarbons, with lubricants accounting for 56% of the product slate and a reduced fraction of C12–C20 products (41%), reflecting the more limited chain scission efficiency associated with highly entangled, long polymer chains (Table S10 and Fig. S16). Notably, PE-RW closely mirrors the behavior of UHMWPE rather than that of PE4000. Despite its heterogeneous nature and the presence of additives, fillers, or copolymeric components, PE-RW achieves a comparable conversion (27%) and predominantly forms lubricant-range hydrocarbons (>C20, 60%), alongside a significant fraction of jet fuel and diesel products (34%) and a minor gasoline contribution (6%). Importantly, gas formation is negligible in all cases, underscoring the high degree of control over the depolymerization process and the absence of extensive over-cracking. It should be emphasized that comparisons between polymers with substantially different molecular weights cannot be interpreted solely on the basis of overall conversion values. From a statistical standpoint, ultra-high molecular weight polyethylene inherently requires a significantly greater number of sequential C–C bond cleavage events per chain to reach the C5–C50 carbon number regime within a

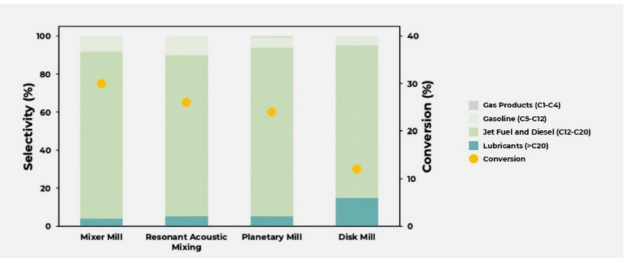

Fig. 4 Comparative performance of four mechanochemical systems for the upcycling of PE4000 in the presence of Ru/Al_2O_3 catalyst and 2-PrOH as H-donor source. Reaction conditions: room temperature, 6 h, PE/Ru mass ratio: 40 : 1, PE/2-PrOH molar ratio: 1 : 100, 1. MM-500 mixer mill: 1 × 10 mm zirconia balls, 30 Hz; P7 planetary mill: 10 × 10 mm zrconia balls, 800 rpm; RAM II resonant acoustic mixer: no milling media, 90 g acceleration; RS 300 disc mill: zirconia disc, default frequency. Reported selectivity refers exclusively to GC-detectable volatile products.

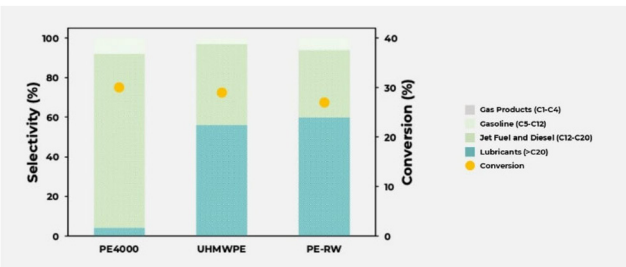

Fig. 5 Comparison of mechanocatalytic upcycling of model PE4000, UHMWPE and real plastic waste promoted by Ru/Al_2O_3 catalyst in the presence of 2-PrOH as H-donor source. Reaction conditions: room temperature, 6 h, PE/Ru mass ratio: 40 : 1, PE/2-PrOH molar ratio: 1 : 100, MM-500 mixer mill: 1 × 10 mm zirconia balls, 30 Hz. Reported selectivity refers exclusively to GC-detectable volatile products.

Open Access Article. Published on 12 Mei 2026. Downloaded on 12/06/2026 20:59:30.
This article is licensed under a Creative Commons Attribution 3.0 Unported Licence.

fixed reaction time. Consequently, differences in product distribution primarily reflect the intrinsic need for multiple catalytic turnovers per macromolecule rather than a variation in catalytic selectivity. The present work is conceived as a systematic comparative evaluation of different substrates processed under identical mechanocatalytic boundary conditions. A rigorous quantification of the average number of C–C cleavages per chain would necessitate complete reconstruction of the product molecular weight distributions together with detailed analysis of the residual polymer fraction, which lies beyond the scope of this study. Such detailed cleavage statistics will be the focus of future dedicated mechanistic investigations. Rather than representing a limitation, these results highlight the intrinsic robustness and adaptability of the catalytic system. The ability to process chemically complex, unrefined plastic waste while maintaining controlled product distributions emphasizes the potential of this approach for practical chemical upcycling. Furthermore, the observed dependence of product selectivity on the initial polymer chain length provides a clear handle for future optimization strategies, including catalyst design and targeted pre-treatments, aimed at steering product slates toward specific fuel or lubricant fractions across diverse waste streams.

Conclusions

This work establishes a novel mechanocatalytic strategy for the selective upcycling of polyethylene, leveraging the dual role of 2-propanol as both hydrogen donor and liquid-assisted grinding (LAG) agent. In combination with Ru/Al_2O_3, 2-propanol enables reductive depolymerization under mild, hydrogen-free conditions. Acting as a LAG medium, it improves polymer mobility and mass transfer during milling, while simultaneously providing *in situ* hydrogen through transfer processes. Systematic optimization revealed that 2-propanol outperforms other secondary alcohols, with product selectivity tunable *via* reaction time. A shift from heavy lubricant range products (>C20) to lighter liquid hydrocarbons (C5–C20) was achieved with minimal gas formation. It should be noted that the liquid product distributions discussed herein are derived from GC–MS analysis, which inherently probes only the volatile and semi-volatile fraction of the reaction mixture. Additional experiments performed under optimized conditions with mixer mill using mesitylene as internal standard confirmed that only a portion of the total products is detectable by GC (Fig. S17). The GC-visible volatile fraction corresponding to C5–C20 products amounted to 0.47 mg under optimized conditions, corresponding to 0.188 wt% relative to the initial polymer mass. Complementary MALDI-TOF analyses further revealed the presence of higher molecular weight species beyond the GC detection range (Fig. S18). Accordingly, the reported selectivity values refer exclusively to GC-detectable compounds and should be interpreted as representative of the volatile product fraction, thus providing a comparative rather than absolute description of the overall product distribution. Importantly, the overall product yield, quantified in mg, is consistent with values reported in recent studies by the Vollmer group,[12,35] further supporting the reliability and relevance of the present methodology. It should be noted that a substantial fraction of the liquid products in the C5–C20 range are oxygenated species (alcohols, ketones, ethers), reflecting the intrinsic radical quenching pathways promoted by 2-propanol under mechanochemical conditions, in addition to its established role as hydrogen donor. It is important to note that the mechanochemical pathway investigated here differs fundamentally from thermocatalytic depolymerization processes. In thermally driven systems, radical formation typically arises from thermal activation of polymer chains or surface-mediated reactions at the catalyst interface. In contrast, under mechanochemical conditions the primary C–C bond cleavage is induced directly by mechanical stress during ball milling, generating macroradicals within the polymer matrix. In this scenario, the Ru/Al_2O_3 catalyst mainly facilitates hydrogen transfer reactions that stabilize the reaction intermediates rather than initiating the bond cleavage step. While the overall polyethylene conversion achieved under mechanochemical conditions is lower than that reported for high-temperature or hydrogen-assisted systems, the present approach operates at ambient temperature and atmospheric pressure and exhibits very high selectivity toward liquid-range products with negligible gas formation. This highlights a fundamental trade-off between conversion and operational mildness, positioning mechanocatalysis as a complementary, rather than competing, strategy to thermally driven PE upcycling routes. Catalyst characterization showed that extended milling times lead to progressive deactivation, due to carbon deposition and abrasion of the zirconia grinding media.

Moreover, this work systematically investigates four mechanocatalytic technologies for the selective upcycling of polyethylene: (i) mixer mill, (ii) planetary mill, (iii) vibratory disc mill, and (iv) resonant acoustic mixer. Among the four mechanochemical platforms tested, the mixer mill delivered the highest conversion and selectivity under optimized conditions. However, the resonant acoustic mixer (RAM) also showed promising performance despite the absence of grinding media, highlighting its potential for scalable and energy-efficient applications.

While most literature examples of mechanokinetic depolymerization of polyolefins produce predominantly very short-chain hydrocarbons or gaseous products,[33–35] the present work demonstrates a clear transition toward the selective formation of liquid-range compounds (Table S11). This shift moves the outcome from species of marginal practical relevance to hydrocarbons directly suitable for fuels and chemical feedstocks. Accordingly, the combination of Ru/Al_2O_3 with 2-propanol not only complements existing strategies but advances the field by bridging the gap between indiscriminate chain fragmentation and controlled product generation.

A broader comparison with previously reported mechanochemical upcycling systems (Table S11) further clarifies the distinctive positioning of this platform. In most literature pre-

 This journal is © The Royal Society of Chemistry 2026

Open Access Article. Published on 12 Mei 2026. Downloaded on 12/06/2026 20:59:30.
This article is licensed under a Creative Commons Attribution 3.0 Unported Licence.

cedents, the product slate is largely confined to C1–C4 or, in more favorable cases, C1–C10 fractions, commonly associated with unselective radical scission pathways. By contrast, the Ru/Al_2O_3/2-propanol system operates through a cooperative interplay between mechanical bond activation and catalytic hydrogen transfer, stabilizing reactive intermediates before secondary overcracking can occur. This controlled interception redirects the reaction network toward C5–C20 hydrocarbons with minimal gas formation under ambient temperature and atmospheric pressure. In this context, the reported selectivity values refer exclusively to GC-detectable volatile products and should be interpreted as relative compositional distributions within this fraction, rather than as absolute yields based on the total converted material. Such integration of mechanochemical activation with catalytic hydrogen management distinguishes the present approach from purely fragmentation-driven methodologies and establishes a pathway to value-added liquid fractions.

Overall, this study demonstrates that combining Ru/Al_2O_3 catalysis with 2-propanol as both LAG agent and hydrogen donor provides a controlled, hydrogen-free route to polyethylene valorization. Beyond identifying key operational parameters and reactor configurations, it lays the foundation for tunable and scalable mechanocatalytic systems, contributing to the development of sustainable strategies for plastics circularity. Notably, catalytic performance is preserved when switching from the model substrate to both a commercial polyethylene characterized by substantially longer chains (ultra-high molecular weight polyethylene) and to real waste polyethylene, underscoring the resilience and flexibility of the mechanocatalytic approach. The differences in product distribution observed for the high molecular weight substrates reflect the inherently greater number of sequential C–C cleavage events required per chain within a fixed milling time, rather than a change in catalytic selectivity. A quantitative assessment of cleavage statistics in different molecular weight regimes will be the subject of future dedicated investigations. Although the extent of conversion depends on factors such as chain length, chemical composition, and morphological features of the polymer, the effective processing of long-chain commercial materials and structurally heterogeneous waste demonstrates that the methodology is applicable well beyond idealized systems.

Author contributions

A. C. P. T. performed all experiments. M. W. performed substrate scope experiments. E. P., A. D., F. M., S. G. and L. B. conceived and designed the research activities. R. P. and E. G. conducted the catalyst synthesis and physico-chemical characterization. All authors discussed results and contributed to the manuscript. All authors approved the final version of the manuscript.

Conflicts of interest

There are no conflicts to declare.

Data availability

The data supporting this article have been included as part of the supplementary information (SI). Supplementary information is available. See DOI: https://doi.org/10.1039/d6py00117c.

Acknowledgements

A. C. P. T. gratefully acknowledge the Mediterranea University of Reggio Calabria and the Italian Ministry of University and Research (MUR) for funding. This publication was prepared with support and funding by the Italian Ministry of University and Research (MUR) within PRIN 2022 project "2022PPXWMS – Catalytic Upcycling of PolyolefIn waste: a matter of awareness (CUPId)". E. G. acknowledge support from Project CH4.0 under the MUR program "Dipartimenti di Eccellenza 2023-2027" (CUP D13C22003520001).

References

1 Plastics Europe, [Online] https://plasticseurope.org/.
2 K. Faust, P. Denifl and M. Hapke, *ChemCatChem*, 2023, **15**, e202300310.
3 J. Sun, J. Dong, L. Gao, Y.-Q. Zhao, H. Moon and S. L. Scott, *Chem. Rev.*, 2024, **124**, 9457–9579.
4 A. C. P. Trimboli, E. Paone, P. Torelli, E. Groppo and F. Mauriello, *Chem Catal.*, 2026, 101662.
5 E. Paone, M. Miceli, A. Malara, G. Ye, E. Mousa, E. Bontempi, P. Frontera and F. Mauriello, *ACS Sustainable Chem. Eng.*, 2022, **10**(7), 2275–2281.
6 A. C. P. Trimboli, V. Bressi, E. Paone, R. Pellegrini, P. Lazzarini, E. C. Groppo and F. Mauriello, *ChemRxiv*, 2025, preprint, DOI: 10.26434/chemrxiv-2025-vsrzv. This content is a preprint and has not been peer-reviewed.
7 E. Jung, D. Yim, H. Kim, G. I. Peterson and T. Choi, *J. Polym. Sci.*, 2023, **61**(7), 553–560.
8 Y. Chang, S. J. Blanton, R. Andraos, V. S. Nguyen, C. L. Liotta, F. J. Schork and C. Sievers, *ACS Sustainable Chem. Eng.*, 2024, **12**(1), 178–191.
9 S. Aydonat, A. H. Hergesell, C. L. Seitzinger, R. Lennarz, G. Chang, C. Sievers, J. Meisner, I. Vollmer and R. Göstl, *Polym. J.*, 2024, **56**, 249–268.
10 M. Mayer, M. Wohlgemuth, A. S. Straub, S. Grätz and L. Borchardt, *Angew. Chem., Int. Ed.*, 2025, **64**, e202424139.
11 M. Wohlgemuth, S. Schmidt, M. Mayer, W. Pickhardt, S. Graetz and L. Borchardt, *Angew. Chem., Int. Ed.*, 2024, **63**, e202405342.
12 A. H. Hergesell, R. J. Baarslag, C. L. Seitzinger, R. Meena, P. Schara, Z. Tomovic, G. Li, B. M. Weckhuysen and I. Vollmer, *J. Am. Chem. Soc.*, 2024, **146**(38), 26139–26147.
13 L. Li, M. Leutzsch, P. Hesse, C. Wang, B. Wang and F. Schüth, *Angew. Chem., Int. Ed.*, 2025, **64**, e202413132.
14 W. Pickhardt, S. Gratz and L. Borchardt, *Chem. – Eur. J.*, 2020, **26**, 12903–12911.

Open Access Article. Published on 12 Mei 2026. Downloaded on 12/06/2026 20:59:30.
This article is licensed under a Creative Commons Attribution 3.0 Unported Licence.

15 A. Stolle, R. Schmidt and K. Jacob, *Faraday Discuss.*, 2014, **170**, 267–286.
16 C. F. Burmeister and A. Kwade, *Chem. Soc. Rev.*, 2013, **42**, 7660–7667.
17 A. Krusenbaum, L. Borchardt, S. Gratz, G. T. Tigineh and J. G. Kim, *Chem. Soc. Rev.*, 2022, **51**, 2873.
18 E. G. Soares, J. Castro-Gomes, M. Sitarz, T. Zdeb, I. Hager, K. Hassan and M. S. Al-Kuwari, *Constr. Build. Mater.*, 2022, **323**, 126488.
19 Z. Jiang, J. Zepper, X. Ling, K. Schollbach and H. J. H. Brouwers, *Cem. Concr. Compos.*, 2024, **150**, 105564.
20 M. Wohlgemuth, S. Schmidt, M. Mayer, W. Pickhardt, S. Grätz and L. Borchardt, *Chem. – Eur. J.*, 2023, **29**, e202301714.
21 L. Gonnet, C. B. Lennox, J.-L. Do, I. Malvestiti, S. G. Koenig, K. Nagapudi and T. Friščić, *Angew. Chem., Int. Ed.*, 2022, **61**, e202115030.
22 R. J. Conk, S. Hanna, J. X. Shi, J. Yang, N. R. Ciccia, L. Qi, B. J. Bloomer, S. Heuvel, T. Wills, J. Su, A. T. Bell and J. F. Hartwig, *Science*, 2022, **377**, 1561–1566.
23 N. M. Wang, G. Strong, V. DaSilva, L. Gao, R. Huacuja, I. A. Konstantinov, M. S. Rosen, A. J. Nett, S. Ewart, R. Geyer, S. L. Scott and D. Guironnet, *J. Am. Chem. Soc.*, 2022, **144**, 18526–18531.
24 W. Zhang, S. Kim, L. Wahl, R. Khare, L. Hale, J. Hu, D. M. Camaioni, O. Y. Gutiérrez, Y. Liu and J. A. Lercher, *Science*, 2023, **379**, 807–811.
25 G. Agostini, E. Groppo, A. Piovano, R. Pellegrini, G. Leofanti and C. Lamberti, *Langmuir*, 2010, **26**(13), 11204–11211.
26 E. Groppo, G. Agostini, A. Piovano, N. B. Muddada, G. Leofanti, R. Pellegrini, G. Portale, A. Longo and C. Lamberti, *J. Catal.*, 2012, **287**, 44–54.
27 P. Lazzarini, D. Bonavia, A. Ricchebuono, E. Seminerio, G. Deplano, R. Pellegrini, L. Braglia, E. Paone, F. Mauriello, S. Checchia, D. Ferri, A. Piovano and E. Groppo, *ACS Catal.*, 2026, **16**(2), 1077–1090.
28 R. Helmer, S. S. Borkar, A. Li, F. Mahnaz, J. Vito, M. Bishop, A. Iftakher, M. M. F. Hasan, S. Rangarajan and M. Shetty, *Angew. Chem., Int. Ed.*, 2025, **64**, e202416384.
29 Y. Nakaji, M. Tamura, S. Miyaoka, S. Kumagai, M. Tanji, Y. Nakagawa, T. Yoshioka and K. Tomishige, *Appl. Catal., B*, 2021, **285**, 119805.
30 M. Tamura, S. Miyaoka, Y. Nakaji, M. Tanji, S. Kumagai, Y. Nakagawa, T. Yoshioka and K. Tomishige, *Appl. Catal., B*, 2022, **318**, 121870.
31 A. Kamali, J. M. Little, S. Luo, A. Chen, A. Warty, A. Bhowmick, J. Moncada, E. P. Jahrman, B. C. Vance, J. K. Keum, T. J. Woehl, P.-Y. Chen, D. G. Vlachos and D. Liu, *Chem Catal.*, 2025, 101459.
32 A. S. Makarov and M. Rueping, *Green Chem.*, 2025, **27**, 716–721.
33 R. Gu, T. Wang, Y. Ma, T.-X. Wang, R.-Q. Yao, Y. Zhao, Z. Wen, G.-F. Han, X.-Y. Lang and Q. Jiang, *Angew. Chem., Int. Ed.*, 2025, **64**, e202417644.
34 L. Li, O. Vozniuk, Z. Cao, P. Losch, M. Felderhoff and F. Schüth, *Nat. Commun.*, 2023, **14**(1), 5257.
35 A. H. Hergesell, C. L. Seitzinger, J. Burg, R. J. Baarslag and I. Vollmer, *RSC Mechanochem.*, 2025, **2**, 263–272.

This journal is © The Royal Society of Chemistry 2026